Helene, C., & Dimicoli, J.-L. (1972) *FEBS Lett. 26*, 6-10.
Hertzberg, R. P., & Dervan, P. B. (1982) *J. Am. Chem. Soc. 104*, 313-315.
Hoffman, D. W., Query, C. C., Golden, B. L., White, S. W., & Keene, J. D. (1991) *Proc. Natl. Acad. Sci. U.S.A. 88*, 2495-2499.
Kawano, K., Yoneya, T., Miyata, T., Yoshikawa, K., Tokunaga, F., Terada, Y., & Iwanaga, S. (1990) *J. Biol. Chem. 265*, 15365-15367.
Krishna, P., Kennedy, B. P., Waisman, D. M., van de Sande, J. H., & McGhee, J. D. (1990) *Proc. Natl. Acad. Sci. U.S.A. 87*, 1292-1295.
Kuwahara, J., & Sugiura, Y. (1988) *Proc. Natl. Acad. Sci. U.S.A. 85*, 2459-2463.
Landschultz, W. H., Johnson, P. F., & McKnight, S. L. (1988) *Science 240*, 1759-1764.
Lane, M. J., Dabrowiak, J. C., & Vournakis, J. N. (1983) *Proc. Natl. Acad. Sci. U.S.A. 80*, 3260-3264.
Lehrer, R. I., Ganz, T., & Selsted, M. E. (1991) *Cell 64*, 229-230.
Low, C. M. L., Drew, H. R., & Waring, M. J. (1984) *Nucleic Acids Res. 12*, 4865-4879.
Mascharak, P. K., Sugiura, Y., Kuwahara, J., Suzuki, T., & Lippard, S. J. (1983) *Proc. Natl. Acad. Sci. U.S.A. 80*, 6795-6798.
Matsuzaki, K., Fukui, M., Fujii, N., & Miyajima, K. (1991) *Biochim. Biophys. Acta 1070*, 259-264.
Maxam, A. M., & Gilbert, W. (1980) *Methods Enzymol. 65*, 499-560.
Miyata, T., Tokunaga, F., Yoneya, T., Yoshikawa, K., Iwanaga, S., Niwa, M., Takao, T., & Shimonishi, Y. (1989) *J. Biochem. (Tokyo) 106*, 663-668.
Morita, F. (1974) *Biochim. Biophys. Acta 343*, 674-681.
Nakamura, T., Furunaka, H., Miyata, T., Tokunaga, F., Muta, T., Iwanaga, S., Niwa, M., Takao, T., & Shimonishi, Y. (1988) *J. Biol. Chem. 263*, 16709-16713.
Pabo, C. O., & Sauer, R. T. (1984) *Annu. Rev. Biochem. 53*, 293-321.
Rafferty, J. B., Somers, W. S., Saint-Girons, I., & Phillips, S. E. V. (1989) *Nature 341*, 705-710.
Scamrov, A. V., & Beabealashvilli, R. Sh. (1983) *FEBS Lett. 164*, 97-101.
Scherly, D., Boelens, W., Dathan, N. A., van Venrooij, W. J., & Mattaj, I. W. (1990) *Nature 345*, 502-506.
Siebenlist, U., & Gilbert, W. (1980) *Proc. Natl. Acad. Sci. U.S.A. 77*, 122-126.
Stubbe, J., & Kozarich, J. W. (1987) *Chem. Rev. 87*, 1107-1136.
Sugiura, Y., & Suzuki, T. (1982) *J. Biol. Chem. 257*, 10544-10546.
Tullius, T. D., Dombroski, B. A., Churchill, M. E. A., & Kam, L. (1987) *Methods Enzymol. 155*, 537-558.
Van Dyke, M. W., & Dervan, P. B. (1983) *Nucleic Acids Res. 11*, 5555-5567.
Van Dyke, M. W., & Dervan, P. B. (1984) *Science 225*, 1122-1127.
Van Dyke, M. W., Hertzberg, R. P., & Dervan, P. B. (1982) *Proc. Natl. Acad. Sci. U.S.A. 79*, 5470-5474.
Wang, A. H.-J., Ughetto, G., Quigley, G. J., Hakoshima, T., van der Marel, G. A., van der Boom, J. H., & Rich, A. (1984) *Science 225*, 1115-1121.
Yang, C.-C., & Nash, H. A. (1989) *Cell 57*, 869-880.

# Identification of Intermolecular RNA Cross-Links at the Subunit Interface of the *Escherichia coli* Ribosome†

Philip Mitchell,* Monika Osswald, and Richard Brimacombe
*Max-Planck-Institut für Molekulare Genetik, Abteilung Wittmann, Ihnestrasse 73, Federal Republic of Germany*
*Received October 11, 1991; Revised Manuscript Received December 20, 1991*

ABSTRACT: $^{32}$P-Labeled 70S ribosomes and polysomes were isolated from cultures of *Escherichia coli* and treated with the cross-linking reagent bis(2-chloroethyl)methylamine. Intermolecular 16S-23S RNA cross-linked complexes were separated from other products of the cross-linking reactions by a two-step sucrose density gradient centrifugation procedure and subjected to oligodeoxynucleotide-directed partial nuclease digestions with RNase H. Cross-linked RNA fragments released by such directed digests were resolved by two-dimensional gel electrophoresis and analyzed using classical oligonucleotide fingerprinting techniques. Two distinct intermolecular cross-links between the 16S and 23S RNA could be localized in this manner, involving positions 1408-1411 and 1518-1520 in the 16S RNA sequence and positions 1912-1920 in the 23S RNA sequence. These data provide the first direct topographical links between the RNA of the 30S and 50S subunits in the functional ribosome and, together with previous topographical data concerning the three-dimensional folding of the rRNA, demonstrate that there is a tight cluster at the ribosomal interface both of sites implicated in ribosomal function and of posttranscriptionally modified nucleotides in the rRNA.

The research efforts of this laboratory have been concentrated on the development and application of cross-linking techniques to obtain detailed information concerning the topography of the 16S and 23S RNA in situ in the *Escherichia coli* ribosome. We have previously reported a large number of intra-RNA and RNA-protein cross-link analyses [summarized by Brimacombe et al. (1990a,b)], and these data sets for 16S and 23S RNA, in conjunction with other topographical information, have been incorporated into a model (Brimacombe et al., 1988a) for the detailed three-dimensional structure of the *E. coli* 16S RNA and, more recently, a model (Mitchell et al., 1990) for the tertiary structure of the tRNA binding domain in 23S RNA from *E. coli*, respectively. In a slightly more

† This work was supported in part by a grant from the Deutsche Forschungsgemeinschaft (SFB 9).

0006-2960/92/0431-3004$03.00/0 

recent model for the folding of 16S RNA (Stern et al., 1988), Noller's group incorporated, in addition to the data used to construct our model, the results of their extensive ribosomal footprinting studies.

Although these models are crude representations of the tertiary structures of the rRNA which remain open to refinement as more topographical data become available [e.g., Stiege et al. (1988) and Döring et al. (1991)], the availability of these structures provides a basis for interpreting data concerning molecular interactions between rRNA and ribosomal ligands, such as mRNA and tRNA. Moreover, with models for both the 16S RNA (Brimacombe et al., 1988a; Stern et al., 1988) and the tRNA binding domain of 23S RNA (Mitchell et al., 1990), we are now able to consider these interactions in terms of the complete translational apparatus, namely, the 70S ribosome.

Central to the integration of the existing models for each individual subunit into a representative structure for the 70S particle is an understanding of the mutual orientation of the subunits themselves. Whereas isolated ribosomal subunits display characteristic shapes when visualized on electron micrographs, 70S ribosomes appear rather globular, with poorly defined structural features. Although a consensus electron microscopy model exists for the arrangement of the 30S and 50S subunits in the 70S particle [e.g., Stöffler-Meilicke and Stöffler (1990) and Frank et al. (1991)], no detailed information at the nucleotide or amino acid level has been hitherto put forward concerning direct points of contact between the ribosomal subunits.

In an earlier publication (Zwieb et al., 1978), we reported the observation of an intermolecular cross-link between 16S and 23S RNA in the *E. coli* ribosome upon treatment of 70S particles with the homobifunctional reagent bis(2-chloroethyl)methylamine (nitrogen mustard), but we were unable to define the sites involved in the cross-link. Using recently developed methodologies for the isolation of individual cross-linked complexes (Stade et al., 1989; Mitchell et al., 1990) developed in this laboratory, we have now been able to localize the principal site of cross-linking to positions 1408–1411 in the 16S RNA and positions 1912–1920 in the 23S RNA. An additional cross-link involving the same site in the 23S RNA and positions 1518–1520 in the 16S RNA was also observed. Furthermore, the same two cross-links were found when polysomes were used as the substrate for the reagent. These new cross-link data allow the mutual orientation of the two subunit models to be "anchored", in a manner which draws together sites in the rRNA previously implicated in ribosomal function into a topographically related group, clustered at the subunit interface of the ribosome.

## Experimental Procedures

$^{32}$P-Labeled "tight couple" 70S ribosomes and polysomes were prepared from cultures of *E. coli* strain MRE 600 using a suitably adapted protocol to our standard procedure (Brimacombe et al., 1988b). After harvesting, the cells were sonicated in a buffer containing 10 mM triethanolamine hydrochloride, pH 7.8, and 10 mM $Mg(OAc)_2$, and after removal of cell debris by centrifugation, the extract was loaded onto a 10–40% sucrose gradient containing 25 mM triethanolamine hydrochloride, pH 7.8, 50 mM KCl, and 6 mM $Mg^{2+}$. Gradient fractions containing tight couple 70S ribosomes and polysomes were pooled separately and made up to 10 mM in $Mg^{2+}$.

Cross-linking reactions were performed directly on ribosomal particles in the sucrose gradient fractions by treatment with 2 mM nitrogen mustard under published conditions (Brimacombe et al., 1988b). The cross-linked ribosomal particles were resolved by sucrose density gradient centrifugation under subunit dissociation conditions (50 mM $K^+$, 0.3 mM $Mg^{2+}$); gradient fractions at the leading edge of the 50S subunit peak (containing 30S–50S cross-linked ribosomes) were pooled and were concentrated by ethanol precipitation. Ribosomal proteins were removed by digestion with proteinase K and extraction with phenol, as described (Brimacombe et al., 1990c).

In preliminary experiments, the isolated cross-linked rRNA or non-deproteinized cross-linked ribosomes were analyzed by gel electrophoresis in a 2.5% polyacrylamide/0.5% agarose gel, using our standard buffer system (Brimacombe et al., 1990c). The 16S–23S RNA cross-linked complex was then detected by autoradiography; the cross-linked samples were compared with non-cross-linked controls run in parallel lanes in the gel. In subsequent experiments, the 16S–23S RNA cross-linked complex was separated from 16S and 23S RNA by centrifugation through a 7.5–30% sucrose density gradient containing 0.1% SDS (Brimacombe et al., 1990c); gradient fractions were collected and analyzed for the presence of the 16S–23S RNA cross-linked complex by gel electrophoresis, as described above. The corresponding gradient fractions were then pooled and the RNA was recovered by precipitation with ethanol in the presence of unlabeled carrier RNA.

Regions of the 16S and 23S RNA containing the site of cross-linking were localized by screening the complete length of the molecules, using RNase H in combination with specific oligodeoxynucleotides, as previously described (Stade et al., 1989; see Results section). The intermolecular cross-links were then isolated as RNA fragment complexes by preparative digestions with RNase H, using sets of oligodeoxynucleotides complementary to the appropriate regions of both 16S and 23S RNA. The cross-linked complexes were isolated by two-dimensional gel electrophoresis (Mitchell et al., 1990), detected by autoradiography, and recovered by extraction of the gel piece in the presence of phenol and subsequent ethanol precipitation (Brimacombe et al., 1990c). Oligonucleotide analyses of the cross-linked complexes and non-cross-linked control fragments were carried out using our standard procedures (Brimacombe et al., 1990c; Döring et al., 1991), and the data obtained were fitted to the published sequences for 16S (Brosius et al., 1978) and 23S (Brosius et al., 1980) RNA.

## Results

Figure 1 shows an autoradiogram of a gel electrophoretic separation of uniformly $^{32}$P-labeled RNA from 70S ribosomes treated with nitrogen mustard. A band corresponding to a high molecular weight species is observed (labeled X-link in Figure 1) which was absent in non-cross-linked control samples, and the intensity of which was shown to increase with increasing concentration of cross-linking reagent (data not shown).

Nitrogen mustard reacts with both RNA and protein; thus, treatment of ribosomal particles with this reagent leads to the concomitant formation of RNA–RNA, RNA–protein, and protein–protein cross-links. However, several lines of evidence lead to the conclusion that the additional band labeled X-link in Figure 1 comprises a direct cross-link between 16S and 23S RNA. First, the involvement of ribosomal protein in the cross-linked complex could be discounted, since extensive digestion of the sample with proteinase K prior to electrophoresis did not alter the observed mobility of the complex. Second, the cross-linked complex could be shown to contain RNA from both the 30S and the 50S ribosomal subunits by using heterogeneous reconstituted 70S particles as the substrate for cross-linking, whereby only one of the two subunits (either 30S or 50S) was radioactively labeled [data not shown; cf.

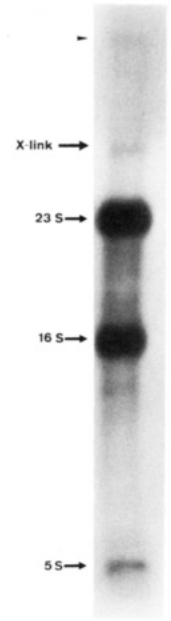


FIGURE 1: Autoradiogram of an electrophoretic separation of RNA from cross-linked ribosomes. $^{32}$P-labeled 70S ribosomes were treated with nitrogen mustard and digested with proteinase K, and the RNA was resolved in a 2.5% polyacrylamide/0.5% agarose gel, as described in Experimental Procedures. The direction of electrophoresis is from top to bottom. The major RNA species are labeled. The additional band, which comprises 16S–23S RNA cross-linked complexes, is denoted by a bold arrow and labeled X-link. The arrowhead at the top of the panel indicates the position of the gel slot.

Zwieb et al. (1978)]. Finally, the cross-linked complex exhibits an electrophoretic mobility consistent with that expected for a complex with the sum of the molecular weights of 16S and 23S RNA. The possibility of an involvement of 5S RNA was eliminated by the subsequent analyses (see below).

Cross-linking reactions were carried out at a low concentration of reagent so as to maximize the probability that the cross-linked complexes analyzed were the products of an initial cross-linking event. Hence, the yield of intermolecular cross-linking observed was rather low (see Figure 1), and in preparative experiments this necessitated the isolation of the cross-linked complex prior to partial nuclease digestion and sequence analysis. This isolation was achieved by two sucrose density gradient centrifugation steps involving first the separation of cross-linked 70S particles from "free" ribosomal subunits, followed by removal of the ribosomal proteins and resolution of the rRNA on a gradient containing SDS. Typical gradient profiles obtained for the preparation of substrates for cross-linking and subsequent isolation of the 16S–23S RNA cross-linked product are shown in Figure 2.

Figure 2A shows the preparation of $^{32}$P-labeled tight couple 70S ribosomes and polysomes by centrifugation through a sucrose gradient containing 6 mM $Mg^{2+}$, as outlined in Experimental Procedures. Gradient fractions containing 70S ribosomes and polysomes (indicated with bars) were pooled separately and subjected to cross-linking with nitrogen mustard. The cross-linked ribosomal particles were then applied to a further sucrose gradient (Figure 2B) under conditions which dissociate free 30S and 50S ribosomal subunits. The nondissociated (cross-linked) ribosomal particles run slightly faster than the large ribosomal subunits, giving rise to the shoulder observed on the 50S peak in Figure 2B. The corresponding gradient fractions (indicated with a bar in Figure 2B) were pooled, and after treatment with proteinase K, the isolated RNA was separated by centrifugation through a final gradient containing SDS. This gradient (Figure 2C) showed three distinct peaks corresponding to 16S, 23S, and the 16S–23S cross-linked complex. Gradient fractions were analyzed by gel electrophoresis in acrylamide/agarose gels (cf. Figure 1), and fractions shown to contain the 16S–23S RNA cross-link free from 23S and 16S RNAs (indicated with a bar in Figure 2C) were pooled for analysis of the sites of cross-linking.

Panels B and C of Figure 2 correspond to the isolation of the cross-linked complex generated upon nitrogen mustard treatment of the 70S peak shown in panel A; however, virtually identical profiles were observed upon analysis of the cross-linked products of the polysome material (data not shown). The yield of cross-linking observed was somewhat variable, and it was of the order of 1%.

A preliminary localization of the sites of cross-linking was performed using the RNase H method previously described (Stade et al., 1989). In this approach, the cross-linked rRNA is subjected to partial nuclease digestions with RNase H in the presence of pairs of oligodeoxynucleotides complementary

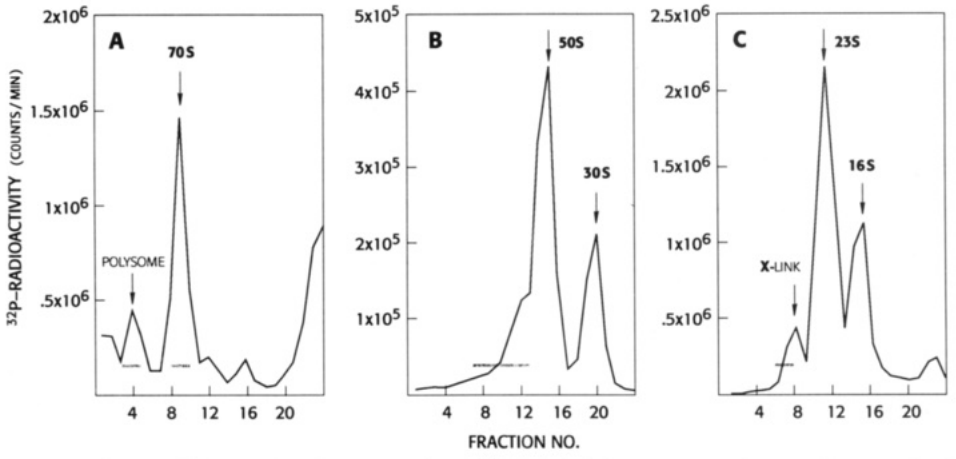


FIGURE 2: Sucrose density gradient profiles showing the preparation of $^{32}$P-labeled ribosomes as substrates for cross-linking reactions and the isolation of the 16S–23S RNA cross-linked product. Panel A: isolation of 70S "tight couple" ribosomes and polysomes on a gradient containing 6 mM $Mg^{2+}$. Gradient fractions indicated by the bars were pooled and treated with cross-linking reagent. Panel B: dissociation of cross-linked ribosomes in a gradient containing 0.3 mM $Mg^{2+}$. Gradient fractions (indicated with a bar) containing nondissociable (cross-linked) ribosomes were pooled, and the RNA was isolated by deproteinization. Panel C: resolution of the cross-linked RNA in a sucrose gradient containing 0.1% SDS. Gradient fractions were analyzed by gel electrophoresis (cf. Figure 1), and those containing only the high molecular weight cross-linked complex (denoted by the bar) were pooled and the RNA was recovered by ethanol precipitation. The direction of sedimentation in each case is from right to left. (Note that the profiles shown in panels A and B were obtained by measuring the radioactivity in aliquots of the gradient fractions, whereas that for panel C shows the complete measured radioactivity for the individual fractions.)

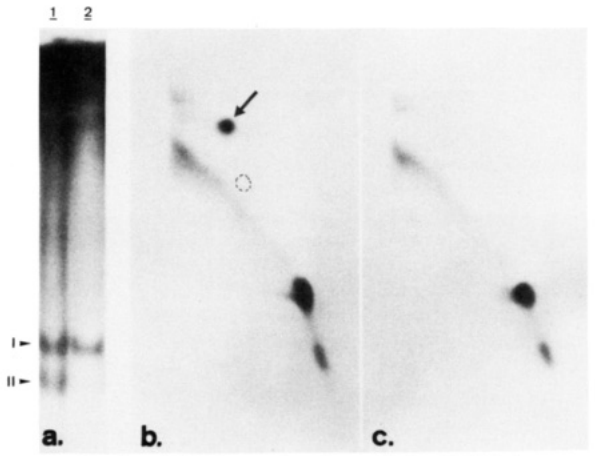


FIGURE 3: Panel a: Gel electrophoretic analysis of RNA fragments released upon digestion with ribonuclease H. Lane 1 contains a digest of a mixture of 16S and 23S RNAs; lane 2 contains the corresponding digest of the 16S–23S RNA cross-linked complex. Digestions were performed with RNase H in the presence of oligodeoxynucleotides complementary to positions 1200–1216 and 1390–1406 in 16S RNA, and the gel was of 5% polyacrylamide (see Experimental Procedures). The direction of electrophoresis is from top to bottom. Bands corresponding to the excised regions of 16S RNA comprising positions ca. 1200–1400 and positions ca. 1400–1542 are denoted I and II, respectively. Panels b and c: two-dimensional gel electrophoretic isolation of an intermolecular RNA cross-linked fragment complex. RNase H digestions were performed using oligodeoxynucleotides complementary to positions 1200–1216 and 1390–1406 in the 16S RNA and positions 1767–1776 and 1962–1971 in the 23S RNA. The direction of electrophoresis is from left to right (5% gel) in the first dimension and from top to bottom (12% gel) in the second dimension. Panel b shows the pattern obtained upon digestion of the 16S–23S RNA cross-linked complex. Panel c shows the control pattern obtained upon digestion of a mixture of 16S and 23S RNA using the same oligodeoxynucleotides The arrow denotes the principal intermolecular cross-linked RNA fragment complex. An additional cross-linked complex was sometimes observed on the two-dimensional gels obtained in other analyses; the running position of this complex is indicated in panel b by a broken circle. The intense spot (lower right) present in both the cross-linked sample and the control sample corresponds to a fragment comprising positions ca. 1200–1400 in the 16S RNA (cf. panel a, band I).

to sites within the 16S or 23S RNA sequence, located approximately 100–200 nucleotides apart. The digestion products are then resolved by electrophoresis in a 5% polyacrylamide gel containing SDS but no urea (Stade et al., 1989). Suitable digestions are performed so as to allow the whole length of each molecule (16S or 23S RNA) to be screened. Control digestions using a stoichiometric mixture of nitrogen mustard treated 16S and 23S RNA isolated from the SDS gradients (cf. Figure 2C) as the substrate were run in parallel. Since in these experiments both the 16S and 23S RNAs are uniformly labeled, digestions of the control samples lead to the release of radiolabeled RNA fragments of low molecular weight comprising the excised regions of the RNA. These fragments are clearly identifiable upon subsequent electrophoretic analysis, being well resolved from fragments comprising other parts of the molecules. A region or regions of the rRNA containing the intermolecular cross-link are thus inferred by the absence of the corresponding low molecular weight fragment upon RNase H digestion of the cross-linked sample, due to its covalent attachment to the (nondigested) complementary rRNA. An example of this screening method is given in Figure 3a.

Figure 3a, lane 1, shows the electrophoretic analysis of a control digest of 16S and 23S RNA with RNase H in the presence of oligodeoxynucleotides complementary to positions 1200–1216 and positions 1390–1406 in 16S RNA. In this instance, one would expect to observe two RNA fragments of low molecular weight, corresponding to positions ca. 1200–1400 and positions ca. 1400 to the 3′-terminus of the 16S RNA. Inspection of Figure 3a (lane 1) shows that this is indeed the case: band I corresponds to positions ca. 1200–1400, whereas band II corresponds to positions ca. 1400–1542. Other regions of the RNA molecule are present in large fragments which remain in the upper regions of the gel.

Figure 3a, lane 2, shows the corresponding digest of the 16S–23S RNA cross-linked complex. In this case, only a single low molecular weight band is visible, corresponding to band I in the control sample (positions ca. 1200–1400). Thus, it can be concluded that the fragment corresponding to positions ca. 1400–1542 is not released from the cross-linked sample due to the presence of a cross-link to the 23S RNA within this region. Digestions of the cross-linked complex using oligodeoxynucleotides complementary to other regions of the 16S RNA showed no differences (with respect to the specifically excised fragments) to the patterns observed in the control samples (data not shown). In a similar set of experiments using oligodeoxynucleotides complementary to sites within the 23S RNA, the cross-link could be localized to positions ca. 1770–1970 in the 23S RNA sequence (data not shown).

Preparative digestions of the intermolecular cross-linked complex were then performed with RNase H, simultaneously using pairs of oligodeoxynucleotides complementary to sites encompassing both the regions in the 16S and 23S RNA identified above. Tne excised cross-linked RNA fragment complexes comprising these regions were isolated by two-dimensional gel electrophoresis (Mitchell et al., 1990) and detected by autoradiography. An example of the two-dimensional gel patterns obtained by this method is given in Figure 3b.

Figure 3b shows an autoradiogram of a two-dimensional gel separation of the products of RNase H digestion of the 16S–23S RNA cross-linked complex in the presence of oligodeoxynucleotides complementary to positions 1200–1216 and 1390–1406 in the 16S and positions 1767–1776 and 1962–1971 in the 23S RNA. Figure 3c shows the corresponding two-dimensional gel pattern obtained upon digestion of a control sample containing a mixture of 16S and 23S RNA (cf. Figure 3a, lane 1). In this gel system, the cross-linked RNA complexes appear as spots above a "diagonal" of non-cross-linked RNA fragments [cf. Döring et al. (1991)], and by using the "directed digest" method with RNase H, the gel patterns observed are very simple [see Mitchell et al. (1990) and Döring et al. (1991)]. In the example given, the diagonal shows only two strong spots, corresponding to positions ca. 1200–1400 in the 16S RNA, and a further fragment, the identity of which was not determined. A spot of high intensity comprising a cross-linked complex (denoted with an arrow) is clearly visible in Figure 3b, but it is absent in the control digest. Cross-links between other regions of the 16S and/or 23S RNAs cannot be ruled out on the basis of these findings. Nonetheless, the strong intensity of the cross-linked fragment identified in Figure 3b indicates that this is the major product of cross-linking between the 16S and 23S RNAs.

The released cross-linked RNA fragments isolated by two-dimensional gel electrophoresis as in Figure 3b were recovered by extraction of the gel pieces in the presence of phenol, and the sites of cross-linking were determined using oligonucleotide analysis techniques. In addition to the major cross-linking products, some of the two-dimensional gels revealed a second rather weaker spot comprising a further

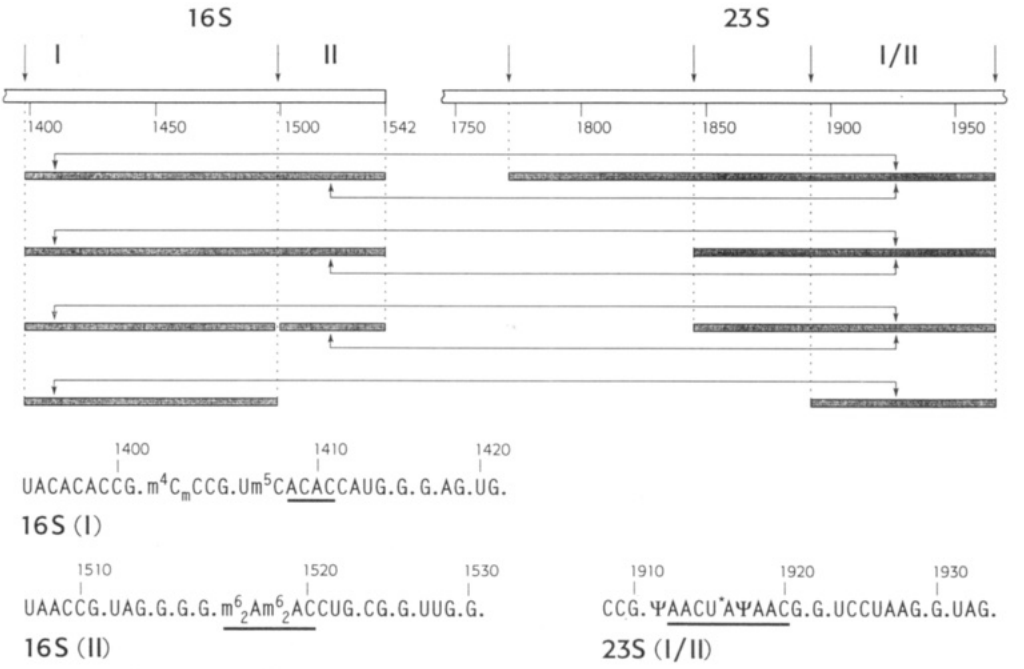


FIGURE 4: Localization of the sites of cross-linking in the 16S–23S RNA cross-linked complexes. The appropriate regions of the 16S and 23S RNA are shown schematically, the arrows denoting sites within these regions that are complementary to the oligodeoxynucleotides used in preparative RNase H digestions. The RNA sequences are numbered from the 5′-end of the molecules. The shaded bars indicate the RNA fragments found in the various cross-linked complexes isolated by gel electrophoresis (cf. Figure 3), the precise sites of cross-linking found by fingerprint analysis being indicated by the double-headed arrows. In the lower part of the Figure the 16S and 23S sequence regions in the vicinity of the two sites of cross-linking are shown, with the identified cross-linked bases underlined. I refers to the major cross-linked product, and II refers to the minor product (cf. Figure 3b). In cases where the 16S fragment spanned both cross-link sites, the two respective complexes were separated on the two-dimensional gel (see Figure 3b). See text for details of the oligonucleotide analyses. (U* at position 1915 in the 23S RNA is an uncharacterized modified uridine residue.)

cross-linked complex; this was not observed in the example shown in Figure 3b, but the position corresponding to its location in other analyses is denoted with a broken circle.

Figure 4 summarizes the results of a number of experiments, in which various combinations of oligodeoxynucleotides were applied so as to progressively "narrow down" the sites of cross-linking and to resolve ambiguities in the fingerprint analyses of the cross-linked complexes [cf. Döring et al. (1991)]. The results of these analyses showed unequivocally that in the major cross-linked product (denoted I in Figure 4) the oligonucleotides Um$^5$CACACCAUGp (positions 1406–1415) in the 16S RNA and ΨAACU*AΨAACGp (positions 1911–1921) in the 23S RNA were missing from the ribonuclease $T_1$ fingerprints. Instead, a new oligonucleotide spot was observed, whose secondary digestion products (with ribonuclease A) were consistent with those expected from a cross-linked complex containing the two "missing" oligonucleotides. Both the ACp spot and the AACp spot in this secondary digest were of reduced intensity, from which it could be concluded that the actual site of cross-linking lay within one of the two AC sequences (positions 1408–1411) of the 16S RNA and within one of the two AAC sequences (positions 1912–1914 and 1918–1920) in the 23S RNA.

In the corresponding analysis of the minor product (II in Figure 4), the same cross-link site in the 23S RNA was found, but in the 16S RNA the oligonucleotide m$^6$Am$^6$ACCUGp (positions 1518–1523) was missing from the $T_1$ fingerprint. The absence of m$^6$Am$^6$ACp (which is clearly distinguishable from AACp) in the secondary digest of the cross-linked oligonucleotide indicated the latter as being the site of cross-linking. Furthermore, both cross-links (I and II) were detected upon analysis of the products of cross-linking of the polysome fractions (Figure 2A) as well as of 70S ribosomes. We therefore conclude that positions 1408–1411 and 1518–1520 in the 16S RNA are in close topographical proximity to positions 1912–1920 in the 23S RNA in the functioning ribosome.

## Discussion

The data presented in these studies provide the missing link between the existing models for 16S (Brimacombe et al., 1988; Stern et al., 1988) and 23S (Mitchell et al., 1990) RNAs, in the construction of models for the three-dimensional arrangement of the rRNA in the 70S ribosome. A number of previous cross-linking investigations have aimed at identifying components at the ribosomal interface but have concentrated upon the identification of ribosomal proteins, involved in either interprotein [e.g., Traut et al. (1986)] or protein–rRNA [e.g., Chiam and Wagner (1983)] cross-links. However, the value of such data in the construction of RNA models is limited by the inherent uncertainties in correlating the three-dimensional arrangement of the rRNA with the known spatial arrangement of the ribosomal proteins (Capel et al., 1988; Walleczek et al., 1988) [for a detailed discussion, see Brimacombe et al. (1990a)]. Moreover, the rather large number of ribosomal proteins implicated as being at the ribosomal subunit interface in the above studies makes a correlation of the data with the protein distributions within the respective subunits (Capel et al., 1988; Walleczek et al., 1988) very difficult.

The locations of the sites of 16S–23S RNA intermolecular cross-linking in the secondary structure models (Brimacombe et al., 1990c; Brimacombe, 1991) for the corresponding regions of the molecules are shown in Figure 5. This figure also includes topographical data concerning interactions between rRNA and ribosomal bound tRNA derived from chemical protection (Moazed & Noller, 1989, 1990) and cross-linking (Prince et al., 1982; Steiner et al., 1988; Wower et al., 1989) studies, as well as the location of known modified nucleotides (Carbon et al., 1979; P. J. Mitchell and B. S. Cooperman, unpublished results), and data from intra-RNA cross-linking

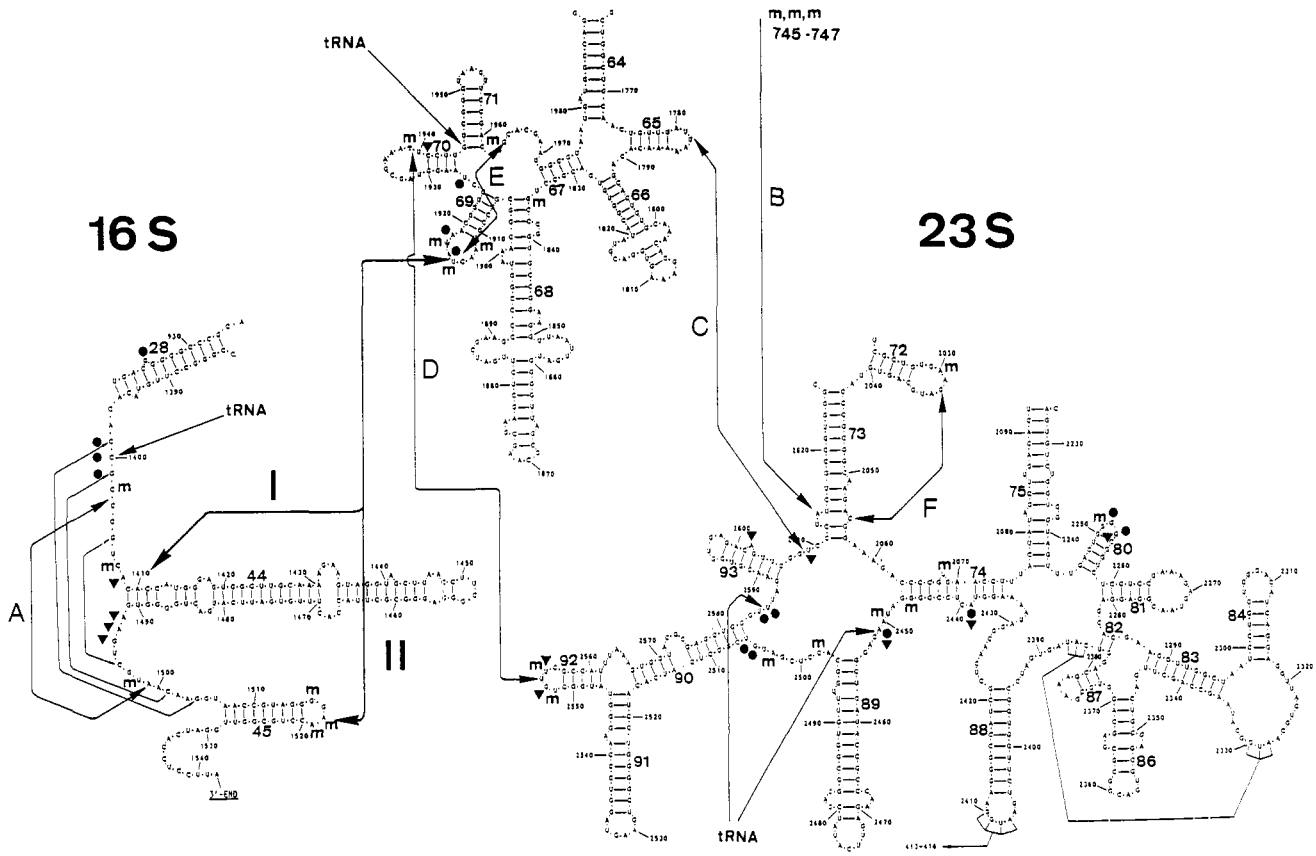


FIGURE 5: Secondary structure models (Brimacombe et al., 1990c; Brimacombe, 1991a) of helices 28, 44, and 45 in the 16S RNA and helices 64–71 and 72–75/80–93 in the 23S RNA. The intermolecular cross-links localized in these studies are denoted by double-headed arrows and are labeled I and II. Nucleotides in these regions which have been implicated in tRNA–ribosome interactions by cross-linking (Prince et al., 1982; Steiner et al., 1988; Wower et al., 1989) or chemical protection (Moazed & Noller, 1989, 1990) studies are indicated: cross-link sites are denoted by arrows and labeled tRNA and footprints of tRNA bound in the ribosomal A- and P-sites are denoted by small triangles and filled circles, respectively. Sites of posttranscriptional modification in the 16S (Carbon et al., 1979) and 23S (P. Mitchell and B. S. Cooperman, unpublished results) RNA are denoted by the symbol m. Intra-RNA cross-linking data (Döring et al., 1991; Brimacombe, 1992) which reveal a topographical cluster of these modified nucleotides in situ in the ribosome are represented by double-headed arrows and are labeled A–F.

experiments [summarized by Döring et al. (1991); T. Döring, B. Greuer, and R. Brimacombe, unpublished results].

Cross-link I involves a nucleotide between positions 1408 and 1411 in the 16S RNA and a site between positions 1912 and 1920 in the 23S RNA. It is of note that sites in this region of the 16S RNA sequence (Brosius et al., 1978) were suggested to lie at the ribosomal subunit interface by the findings of early chemical protection studies (Herr et al., 1978). More recently, nucleotides at the base of helix 44 have been consistently implicated in subunit interactions through protection studies using a variety of chemical probes [e.g., Baudin et al. (1989) and Gornicki et al. (1989)]. Furthermore, in vitro mutagenesis studies (Rottmann et al., 1988) have demonstrated that a point mutation at position 1416 in the 16S RNA inhibits ribosomal subunit association. The analysis of cross-link I now shows unequivocally that the base of helix 44 is at the ribosomal interface and lies in intimate contact with the 23S RNA in the ribosome. Hence, the location of this helix toward the solvent side of the 30S subunit in our current model (Brimacombe et al., 1988a) is clearly incorrect and requires relocation toward the interface side of the 30S subunit, as tentatively proposed by Noller and colleagues (Stern et al., 1988).

Cross-link II involves the identical RNase $T_1$ oligonucleotide in the 23S RNA sequence comprising cross-link I and a distinct site in the 16S RNA, viz., positions 1518–1520 at the loop end of helix 45 (Figure 5). Nucleotides in this region of the 16S RNA have also been previously implicated in ribosomal subunit interactions through chemical protection studies. Indeed, a striking correlation exists between the cross-link analyses reported here and the data of Gornicki et al. (1989). These authors observed clustered protections against cleavage of 16S RNA with $Pb^{2+}$ ions upon binding of 50S subunits to 30S/$tRNA^{Phe}$/poly U complexes, localized at the base of helix 44 and the loop end of helix 45.

It is of note that the 16S RNase $T_1$ oligonucleotide involved in cross-link II contains the universally conserved two adjacent dimethyladenosine residues, which have been previously shown to be involved in ribosomal subunit interaction (Poldermans et al., 1980). Furthermore, both the loop ends of helix 45 in the 16S RNA and helix 69 in the 23S RNA contain no less than three modified nucleotides (see Figure 5). Taken together, cross-links I and II bring these sites to the base of helix 44. This region of the 16S RNA adopts a highly ordered conformational arrangement in situ in the ribosome, as evidenced by the phylogenetically established tertiary interactions (Haselman et al., 1989) between positions 1399/1504, 1401/1501, and 1405/1496 and the intra-RNA cross-link A (Figure 5) between positions 1402–1405 and 1498–1504 (T. Döring, B. Greuer, and R. Brimacombe, unpublished results). An additional three modified nucleotides (positions 1402, 1407, and 1498) are located in this region of the 16S RNA, as is position C-1400. This latter site is generally considered as a "marker" nucleotide for the ribosomal decoding center through the well-established cross-link with the 5'-nucleotide of the P-site bound tRNA anticodon (Prince et al., 1982); tRNA footprints are also located in this area (Moazed & Noller, 1990). It follows that the modified nucleotides noted above form a "nest" at the base of helix 44, in the immediate vicinity

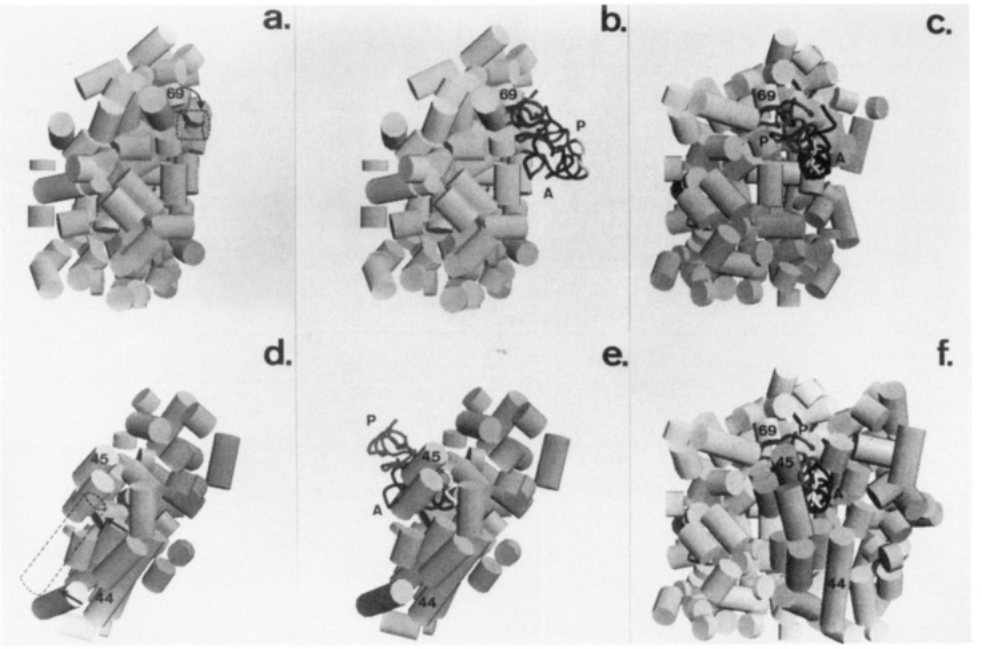


FIGURE 6: Computer model for 16S and 23S RNA [cf. Brimacombe et al. (1988, 1991), and Mitchell et al. (1990)] with P- and A-site bound tRNA. Helical regions in the 16S and 23S RNA are represented as cylinders; the tRNA molecules are shown as phosphate backbone models, the A-site tRNA being more heavily shaded than the P-site tRNA. Helices 44 and 45 in the 16S RNA and helix 69 in the 23S RNA are labeled: note that helices 44 and 45 are directed with their loop ends pointing downward, as viewed, whereas helix 69 is directed with its loop end pointing upward. Panel a: 23S model, viewed from the L1 protuberance side of the 50S subunit. Panel b: as panel a, showing tRNA molecules in the P- and A-sites. Panel c: as panel b, but viewed with the anticodon loops of the tRNA molecules (shown in white) directed toward the viewer. Panel d: 16S RNA model, viewed from the platform side of the 30S subunit. Panel e: as panel d, with two tRNAs. Panel f: model of 16S and 23S RNAs, together with two tRNA molecules, viewed from the same angle as in panel c. Realignments of helices 44 and 69 to allow incorporation of cross-links I and II (see Figure 5) into the model are indicated in panels a and d, their positions being shown by the cylinders drawn in broken lines.

of the site of interaction with the anticodon loop of tRNA. Indeed, several lines of evidence suggest that the remaining methyl groups in 16S RNA (positions 527, 973, 974, and 1207) may well be located nearer to the decoding site than has been hitherto supposed (Brimacombe, 1992).

A similar correlation between the topographical distribution of modified nucleotides and sites associated with tRNA binding is observed in the case of the 23S RNA (see Figure 5). Modified nucleotides and tRNA footprint sites (Moazed & Noller, 1989) are grouped in two regions of the secondary structure, namely the two "ring" structures connecting helices 67–71 and connecting helices, 73, 74, 89, 90, and 93, respectively. Both regions have been shown to be at, or close to, the peptidyltransferase center by cross-linking studies using photoaffinity labels attached to the aminoacyl moiety of Phe-tRNA (Steiner et al., 1988) or incorporated into the 3′-terminal nucleotide of $tRNA^{Phe}$ (Wower et al., 1989; see Figure 5). Indeed, these two regions of the 23S RNA have been directly shown to be in close contact in situ in the 50S subunit by intra-RNA cross-linking studies (Stiege et al., 1983; Mitchell et al., 1990) (cross-links C and D, Figure 5). Additional modified nucleotides in other regions of the secondary structure are shown to be in close proximity with these regions through intra-RNA cross-links B, D, and F. Only one modified nucleotide ($m^6A$-1618, not shown in Figure 5) is not directly linked with this cluster; this site lies in a region of the secondary structure for which there is at present insufficient data to determine whether or not it is spatially related to the other sites.

Local tertiary interactions in the tRNA binding domain of 23S RNA are demonstrated by intra-RNA cross-links between positions 1911–1921 and 1960–1968 (cross-link E, Figure 5), 1931–1933 and 1960–1968, and 1936–1945 and 1964–1965 (Mitchell et al., 1990; Döring et al., 1991). Taken together, cross-links I, A, and E, the cross-link between C-1400 and the anticodon loop of tRNA (Prince et al., 1982), and the cross-link between G-1945 and the 3′-terminal A residue of tRNA (Wower et al., 1989) present the apparent paradox of a close proximity between the anticodon loop and the aminoacyl stem of ribosomal bound tRNA. These structural features of the tRNA molecule lie approximately 70 Å apart in the well-established crystal structure [e.g., Holbrook et al. (1978)]. However, the precise distances between the nucleotides involved in the direct "zero-length" rRNA–tRNA cross-links (C-1400 and G-1945) mentioned above and those involved in the intermolecular cross-links (1408–1411, and 1912–1920, respectively) cannot be deduced from these studies; it must be borne in mind that there are several intervening internucleotide distances and that the cross-linking reagent itself has a length of approximately 8 Å. Moreover, the available data from our cross-linking studies cannot differentiate between various conformations of functionally important regions of the rRNA that are adopted during different stages of the ribosomal elongation cycle. Thus, different cross-links may reflect topographical neighborhoods during different ribosomal functional states. Nevertheless, the intermolecular RNA cross-links analyzed in these studies clearly demonstrate a direct topographical link between the two functional centers of mRNA decoding and peptide bond formation, whereby the spatial distribution of the overwhelming majority, if not all, of the sites of rRNA modification reflects a topographical cluster congruent with the tRNA binding site of the ribosome. Precisely such an RNA bridge connecting the platform of the 30S subunit and the base of the L1 protuberance of the 50S subunit was observed in a recent electron microscopy study (Frank et al., 1991) using three-dimensional image reconstruction techniques of ice-embedded 70S ribosomes (cf. Figure 6).

In a recent study (Brimacombe et al., 1991), we proposed a three-dimensional model for the arrangement of tRNA bound in the P- and A-site of the *E. coli* ribosome. The model was based upon a detailed stereochemical analysis of the mutual orientation of two tRNA molecules in the ribosomal P- and A-sites (V. Lim, C. Venclovas, A. Spirin, F. Müller, P. Mitchell, and R. Brimacombe, manuscript in preparation), our current models (Brimacombe et al., 1988; Mitchell et al., 1990) for the tertiary structure of rRNA in the ribosome, and topographical data available (Prince et al., 1982; Wower et al., 1989) from cross-linking studies on the tRNA–ribosome complex. Views of the model, showing the alignment of tRNA on the 50S subunit, on the 30S subunit, and in the 70S ribosome, are shown in Figure 6.

It is satisfying to note that the intermolecular cross-link data provided by these studies could be readily incorporated into the existing 70S model through minor adjustments of helix 44 in the 16S RNA (see Figure 6d) and helix 69 in the 23S RNA (see Figure 6a), without severe perturbations of other portions of the model. Such rearrangements as shown in Figure 6a,d would have the effect of bringing the loop end of helix 69 and the base of helix 44 together with the loop end of helix 45 (in the 16S RNA) into juxtaposition at a site which defines a direct mutual alignment of the 16S and 23S RNA models. [It should be noted, however, that other parts of the 16S RNA model are currently under review (Brimacombe, 1992)].

## References


Baudin, F., Mougel, M., Romby, P., Eyermann, F., Ebel, J.-P., Ehresmann, B., & Ehresmann, C. (1989) *Biochemistry 28*, 5847–5855.

Brimacombe, R. (1991) *Biochimie 73*, 927–936.

Brimacombe, R. (1992) *Biochimie* (in press).

Brimacombe, R., Atmadja, J., Stiege, W., & Schüler, D. (1988a) *J. Mol. Biol. 199*, 115–136.

Brimacombe, R., Stiege, W., Kyriatsoulis, A., & Maly, P. (1988b) *Methods Enzymol. 164*, 287–309.

Brimacombe, R., Greuer, B., Mitchell, P., Osswald, M., Rinke-Appel, J., Schüler, D., & Stade, K. (1990a) in *The Ribosome: Structure, Function and Evolution* (Hill, W., et al., Eds.) pp 93–106, ASM Press, Washington, DC.

Brimacombe, R., Gornicki, P., Greuer, B., Mitchell, P., Osswald, M., Rinke-Appel, J., Schüler, D., & Stade, K. (1990b) *Biochim. Biophys. Acta 150*, 8–13.

Brimacombe, R., Greuer, B., Gulle, H., Kosack, M., Mitchell, P., Osswald, M., Stade, K., & Stiege, W. (1990c) in *Ribosomes and Protein Synthesis: A Practical Approach* (Spedding, G., Ed.) pp 131–159, IRL Press, Oxford.

Brimacombe, R., Mitchell, P., & Müller, F. (1991) in *Ribosomal RNA: Structure, Evolution, Processing and Function in Protein Synthesis* (Zimmermann, R. A., & Dahlberg, A. E., Eds.) (in press), Telford Press, Caldwell, NJ.

Brosius, J., Palmer, M. L., Kennedy, P. J., & Noller, H. F. (1978) *Proc. Natl. Acad. Sci. U.S.A. 75*, 4801–4805.

Brosius, J., Dull, T. J., & Noller, H. F. (1980) *Proc. Natl. Acad. Sci. U.S.A. 77*, 201–204.

Capel, M. S., Kjeldgaard, M., Engelman, D. M., & Moore, P. B. (1988) *J. Mol. Biol. 200*, 65–87.

Carbon, P., Ehresmann, C., Ehresmann, B., & Ebel, J.-P. (1979) *Eur. J. Biochem. 100*, 399–410.

Chiam, C. L., & Wagner, R. (1983) *Biochemistry 22*, 1193–1200.

Döring, T., Greuer, B., & Brimacombe, R. (1991) *Nucleic Acids Res. 19*, 3517–3524.

Frank, J., Penczek, P., Grassucci, R., & Srivastava, S. (1991) *J. Cell Biol. 115*, 597–605.

Gornicki, P., Baudin, F., Romby, P., Wiewiorowski, M., Kryzosiak, W., Ebel, J.-P., Ehresmann, C., & Ehresmann, B. (1989) *J. Biomol. Struct. Dyn. 6*, 971–984.

Haselman, T., Gutell, R. R., Jurka, J., & Fox, G. E. (1989) *J. Biomol. Struct. Dyn. 7*, 181–186.

Herr, W., Chapman, N. M., & Noller, H. F. (1979) *J. Mol. Biol. 130*, 433–449.

Holbrook, S. R., Sussman, J. L., Warrant, R. W., & Kim, S.-H. (1978) *J. Mol. Biol. 123*, 631–660.

Mitchell, P., Osswald, M., Schüler, D., & Brimacombe, R. (1990) *Nucleic Acids Res. 18*, 4325–4333.

Moazed, D., & Noller, H. F. (1989) *Cell 57*, 585–597.

Moazed, D., & Noller, H. F. (1990) *J. Mol. Biol. 211*, 135–145.

Poldermans, B., Bakker, H., & Van Knippenberg, P. H. (1980) *Nucleic Acids Res. 8*, 143–151.

Prince, J. B., Taylor, B. H., Thurlow, D. L., Ofengand, J., & Zimmermann, R. A. (1982) *Proc. Natl. Acad. Sci. U.S.A. 79*, 5450–5454.

Rottermann, N., Kleuvers, B., Atmadja, J., & Wagner, R. (1988) *Eur. J. Biochem. 177*, 81–90.

Stade, K., Rinke-Appel, J., & Brimacombe, R. (1989) *Nucleic Acids Res. 17*, 9889–9908.

Steiner, G., Kuechler, E., & Barta, A. (1988) *EMBO J. 7*, 3949–3955.

Stern, S., Weiser, B., & Noller, H. F. (1988) *J. Mol. Biol. 204*, 447–481.

Stiege, W., Glotz, C., & Brimacombe, R. (1983) *Nucleic Acids Res. 16*, 4315–4329.

Stiege, W., Kosack, M., Stade, K., & Brimacombe, R. (1988) *Nucleic Acids Res. 16*, 4315–4329.

Stöffler-Meilicke, M., & Stöffler, G. (1990) in *The Ribosome: Structure, Function and Evolution* (Hill, W., Dahlberg, A., Garrett, R., Moore, P., Schlessinger, D., & Warner, J., Eds.) pp 123–133, ASM Press, Washington, DC.

Traut, R. R., Tewari, D. S., Sommer, A., Gavino, G. R., Olson, H. M., & Glitz, D. G. (1986) in *Structure, Function and Genetics of Ribosomes* (Hardesty, B., & Kramer, G., Eds.) pp 286–308, Springer-Verlag, New York.

Walleczek, J., Schüler, D., Stöffler-Meilicke, M., Brimacombe, R., & Stöffler, G. (1988) *EMBO J. 7*, 3571–3576.

Wower, J., Hixson, S. S., & Zimmermann, R. A. (1989) *Proc. Natl. Acad. Sci. U.S.A. 86*, 5232–5236.

Zwieb, C., Ross, A., Rinke, J., Meinke, M., & Brimacombe, R. (1978) *Nucleic Acids Res. 5*, 2705–2720.